Chapter Six

Adjustment under Gravity of a Density-Stratified Fluid

6.1 Introduction

Chapter 5 provided an introduction to the study of adjustment to equilibrium under gravitational forces in the absence of rotation. Attention was restricted, however, to the case of a fluid of uniform density with gravitational restoring forces coming into play when the free surface was perturbed from the horizontal. In this chapter, the study is extended to fluids of variable density.

As a first introduction to the effects of stratification, the case of two superposed shallow layers, each of uniform density, is considered in Sections 6.2 and 6.3. This serves to introduce the concepts of barotropic and baroclinic modes and two widely used approximations: the rigid lid approximation and the Boussinesq approximation. "Shallow" in this case means that the depth of each layer is small compared with the horizontal scale of the perturbation, i.e., the horizontal scale is large compared with the vertical scale.

In reality, of course, the atmosphere and ocean are continuously stratified, although the two-layer model can be quite useful and appropriate for many situations. The study of continuously stratified fluids begins in Section 6.4 with the case of an *incompressible* fluid, i.e., one whose density depends on temperature and composition but not on pressure. No restriction on scale is made at first, but toward the end of the chapter (from Section 6.11 on) special consideration is given to the case in which the horizontal scale is large compared with the vertical scale. This is partly to prepare the way for the introduction of rotation effects in Chapter 7, for with the exception of some rather special situations, rotation is important only for motions with this

property. An additional reason is that most energy in the atmosphere and ocean is in components with this property.

No scale restriction applies to the motions studied in Sections 6.4–6.10. In Section 6.4, the equations for the general case are obtained and the buoyancy frequency N, which is of fundamental importance to the subject, is introduced. The perturbations have a wavelike behavior, the waves concerned being called internal gravity waves. Their most basic properties are most readily studied in the case for which N is constant and the Boussinesq approximation is made. This case is treated in Sections 6.5–6.7. In particular, the "polarization relations" for a plane wave are found in Section 6.5, dispersion properties are discussed in Section 6.6, and energetics in Section 6.7.

It is then but a small step to consider internal waves generated at a (slightly perturbed) horizontal boundary, and this is done in Section 6.8. A particular case of interest is that of waves generated by flow of uniform velocity U over a gently undulating surface. For small-wavelength undulations (wavenumber k greater than N/U), the fluid is only significantly perturbed within a certain distance of the ground, but for large-wavelength undulations ($kU < N$), waves are produced that propagate energy and momentum to large distances from the generating surface.

In practice, the buoyancy frequency N is not uniform, so some important effects of variations in N are considered in Section 6.9, with special reference to the simple case in which N is piecewise uniform. In particular, waves can be refracted and reflected from a discontinuity in N. This can lead to wave energy being confined or "trapped" in a particular structure that is called a duct or waveguide. This concept is applied to free wave propagation in Section 6.10, where methods of treating the general case (N is any function of vertical coordinate z) are developed.

In Section 6.11, there is a return to discussion of cases for which the "hydrostatic approximation" applies, i.e., for which the horizontal scale is large compared with that of the vertical. This serves as a prelude to consideration of adjustment problems rather like that considered in Section 5.6 for the homogeneous case, except that the initial perturbation is now a function of z. However, there is some dependence on the nature of the boundaries. In Section 6.12, we consider adjustment in a semi-infinite region, i.e., a case such as the atmosphere, in which there is a solid boundary below but no definite boundary above. In Section 6.13, we deal with a region of finite depth such as the ocean. The structure of these solutions is of special interest because the way in which they are modified by rotation effects will be considered in Chapter 7.

In Section 6.14, effects of compressibility are considered. For problems of adjustment under gravity, the main new effect of interest is connected with waves that carry energy most rapidly in the horizontal in the atmosphere. These are called Lamb waves, whose vertical scale is the "scale height" and which propagate horizontally at the speed of sound. They were responsible for carrying the pressure pulses observed all around the world following the eruption of Krakatoa, and more recently from nuclear explosions. An example of adjustment in a compressible atmosphere is considered in Section 6.15, and weak dispersion effects, which characterize pressure pulses from distant sources, are considered in Section 6.16. This section, and many others in the book, can be regarded as fairly general discussions of wave properties. Wave dispersion, for instance, is first treated in Section 6.6, and the behavior of waves

in a medium of variable properties is discussed in Section 6.9. Further aspects of wave behavior are to be found in Chapter 8.

When the hydrostatic equation is valid, i.e., when horizontal scales are large compared with vertical scales, it is often advantageous to use pressure as an independent variable in place of height. In particular, the continuity equation has a simple form even when the fluid is compressible. The equations in isobaric coordinates are derived in Section 6.17 and are used later in the book, particularly in connection with slow adjustment processes in the atmosphere (Chapter 12). The energy equations in these coordinates are discussed in Section 6.18.

6.2 The Case of Two Superposed Fluids of Different Density

As a first example of stratification effects, consider the case of two fluids of different density that are immiscible or for which the effect of mixing can be ignored. This system is easily set up in the laboratory, and Marsigli's experiment is an early example. The hydrostatic approximation will be made from the outset, so the results should be applied only to cases in which the horizontal scale is large compared with the depth. The problem was first treated by Stokes (1847).

The means of describing the situation is shown in Fig. 6.1. Subscript 1 is used for the upper layer whose density is ρ_1, whose equilibrium depth is H_1, and whose horizontal velocity components are u_1 and v_1. The free surface, whose equilibrium position is $z = 0$, has perturbed position $z = \eta$. The interface displacement (upward) is h. It follows from the hydrostatic equation

$$\partial p/\partial z = -\rho g \tag{6.2.1}$$

and the surface condition $p = 0$, that the pressure p_1 in the upper layer is given by

$$p_1 = \rho_1 g(\eta - z), \qquad -H_1 + h < z < \eta. \tag{6.2.2}$$

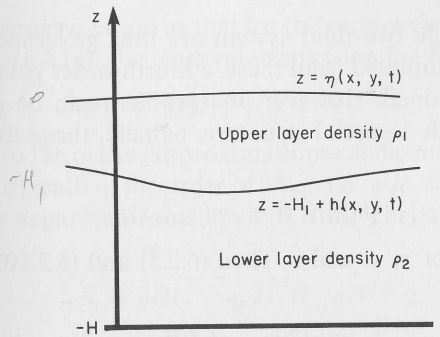

Fig. 6.1. The notation used to describe the motion of two superposed shallow homogeneous layers of fluid. H_1, H_2 are the depths of the layers when at rest and $H = H_1 + H_2$ is the total depth. The z axis points vertically upward, $z = \eta(x, y, t)$ is the surface elevation, and $z = -H + h(x, y, t)$ gives the disturbed position of the interface between the two fluids.

Therefore the momentum equations (4.5.7) and (4.5.8) for small disturbances become

$$\partial u_1/\partial t = -g\,\partial\eta/\partial x, \qquad \partial v_1/\partial t = -g\,\partial\eta/\partial y, \tag{6.2.3}$$

whereas the continuity equation obtained by the same method as that for (5.6.7) is

$$\partial(\eta + H_1 - h)/\partial t + H_1(\partial u_1/\partial x + \partial v_1/\partial y) = 0. \tag{6.2.4}$$

Taking the time derivative and substituting from (6.2.3) for $\partial u_1/\partial t$ and $\partial v_1/\partial t$ eliminate u_1 and v_1 to give

$$\frac{\partial^2}{\partial t^2}(\eta - h) = H_1\left(\frac{\partial^2}{\partial x^2} + \frac{\partial^2}{\partial y^2}\right)g\eta \equiv gH_1\,\nabla^2\eta, \tag{6.2.5}$$

where ∇^2 is defined by (4.3.9).

Similarly, for the lower layer, denoted by subscript 2, the pressure p_2 obtained by integrating (6.2.1) and using continuity of pressure at the interface is

$$p_2 = \rho_1 g(\eta + H_1 - h) + \rho_2 g(-H_1 + h - z), \qquad z < -H_1 + h. \tag{6.2.6}$$

Thus the momentum equations are

$$\frac{\partial u_2}{\partial t} = -\frac{\rho_1}{\rho_2}g\frac{\partial\eta}{\partial x} - g'\frac{\partial h}{\partial x}, \qquad \frac{\partial v_2}{\partial t} = -\frac{\rho_1}{\rho_2}g\frac{\partial\eta}{\partial y} - g'\frac{\partial h}{\partial y}, \tag{6.2.7}$$

where g' is the *reduced gravity* [see (5.1.1)], defined by

$$g' = g(\rho_2 - \rho_1)/\rho_2. \tag{6.2.8}$$

The continuity equation for the layer in this case is

$$\partial h/\partial t + H_2(\partial u_2/\partial x + \partial v_2/\partial y) = 0. \tag{6.2.9}$$

As before, the velocity components are eliminated from these equations to give

$$\frac{\partial^2 h}{\partial t^2} = H_2\left(\frac{\partial^2}{\partial x^2} + \frac{\partial^2}{\partial y^2}\right)\left(\frac{\rho_1}{\rho_2}g\eta + g'h\right) = H_2\,\nabla^2(g\eta - g'\eta + g'h), \tag{6.2.10}$$

use being made of (6.2.8).

The adjustments of the two-fluid system are thus governed by Eqs. (6.2.5) and (6.2.10). If, say, η were eliminated from these, a fourth-order partial differential equation for h would be obtained. However, the problem can be greatly simplified by looking for solutions with a special structure, namely, those for which η and h are proportional, i.e.,

$$h(x, y, t) = \mu\eta(x, y, t), \tag{6.2.11}$$

where μ is independent of x, y, and t. Then (6.2.5) and (6.2.10) both reduce to the second-order equation

$$\partial^2\eta/\partial t^2 = c_e^2\,\nabla^2\eta, \tag{6.2.12}$$

provided that μ and c_e^2 satisfy

$$gH_1/(1 - \mu) = \mu^{-1}(g - g'(1 - \mu))H_2 = c_e^2. \tag{6.2.13}$$

This simplification is an example of a method that can be used for a wide class of mechanical problems involving small oscillations. In fact, Lamb (1932), in his treatise *Hydrodynamics*, spends the first section of his chapter on tidal waves discussing the general theory because of its wide applicability. For the present problem, there are two values of μ, and hence two values of c_e that satisfy the above equation, and the motions corresponding to these particular values are called normal modes of oscillation. In a system consisting of n layers of different density, there are n such modes corresponding to the n degrees of freedom. A continuously stratified fluid corresponds to an infinite number of layers, and so there is an infinite set of modes. The fact that each mode behaves independently is of great utility, and application of the concept will be made repeatedly. The independence of each mode can be seen from the fact that if h and η satisfy (6.2.11) at some initial time, they will then satisfy (6.2.11) for all subsequent times, so only one mode will be in oscillation. If, on the other hand, any given initial state can be represented as a sum of modes the change of each in time and space can be followed independently. The fluid state can then be found by adding together the contributions of each mode.

The structure of the modes is obtained by solving the quadratic (6.2.13) [cf. Stokes (1847, Section 17)], which can be written in the alternative form

$$c_e^4 - gHc_e^2 + gg'H_1H_2 = 0, \tag{6.2.14}$$

where

$$H = H_1 + H_2 \tag{6.2.15}$$

is the total depth of fluid in the equilibrium state. To each of the two solutions (or *eigenvalues*) c_e^2 of (6.2.14) there corresponds a particular normal-mode structure represented by (6.2.11) and the appropriate value of μ. For the case of several layers, there is a value μ_i corresponding to the displacement h_i of each interface, so μ represents an *eigenvector* of the problem.

Another way of expressing the equivalence between the normal mode of the two-layer system and the motion of the one-layer system is to define an *equivalent depth* H_e by

$$c_e^2 = gH_e. \tag{6.2.16}$$

Then η_e satisfies the same equation as that for the surface elevation in a homogeneous fluid of depth H_e. By (6.2.14), the eigenvalue equation for H_e is

$$gH_e^2 - gHH_e + g'H_1H_2 = 0. \tag{6.2.17}$$

For applications to the ocean, approximations can be made because the fractional changes in density are small: of the order of $3^0/_{00}$, i.e., $g'/g = 1 - \rho_1/\rho_2 \approx 0.003$. This results in two widely separated roots c_e^2 of (6.2.14). The larger one, c_0^2, is given approximately by

$$c_0^2 = gH(1 - g'H_1H_2/gH^2\cdots), \tag{6.2.18}$$

and the ratios η/h and u_2/u_1 are approximately

$$\eta/h \approx H/H_2, \qquad u_2/u_1 = 1 - g'H_1/gH\cdots. \tag{6.2.19}$$

In the limit as $g'/g \to 0$, this becomes the surface gravity wave obtained for a fluid

of uniform density. It is often called the *barotropic* mode. The strict meaning of the term "barotropic" is that the pressure is constant on surfaces of constant density, and hence is constant on the interface. This is only approximately true, but it is conventional to call this mode barotropic nevertheless.

The smaller root c_1^2 of (6.2.14) is given for small g'/g by

$$c_1^2 = (g'H_1H_2/H)(1 + g'H_1H_2/gH^2 \cdots), \tag{6.2.20}$$

and the corresponding values of the ratios η/h and u_2/u_1 are approximately

$$\eta/h \approx -g'H_2/gH, \qquad u_2/u_1 \approx -H_1/H_2. \tag{6.2.21}$$

This mode is called the *baroclinic* mode, the word "baroclinic" meaning that pressure is not constant on surfaces of constant density. Typical values of c_1 for the ocean are 2 or 3 m s^{-1}, corresponding to an equivalent depth of 0.5–1 m. Use of the two-layer model for the atmosphere is not so common, but on occasions when it is used, c_1 typically has values of 10–20 m s^{-1} and the equivalent depth of 10–50 m. Often one layer is deep compared with the other, e.g., $H_2 \gg H_1$, and then (6.2.20) is approximated by

$$c_1^2 \approx g'H_1. \tag{6.2.22}$$

Then the internal wave is just the same as a surface gravity wave would be if the acceleration due to gravity were g' instead of g. This is because it is g' that determines pressure differences rather than g (see Section 5.1).

Because $g' \ll g$, the wave speed of internal waves is very much less than that of surface waves, so that the internal waves look like surface waves in slow motion. This difference accounts for a phenomenon noted by Benjamin Franklin (1762, p. 438) in a letter dated December 1, 1762.

> At Madeira we got oil to burn, and with a common glass tumbler or beaker, slung in wire, and suspended to the ceiling of the cabbin .... I made an Italian lamp.... The glass at bottom contained water to about one third of its height; another third was taken up with oil .... At supper, looking on the lamp, I remarked that tho' the surface of the oil was perfectly tranquil, and duly preserved its position with regard to the brim of the glass, the water under the oil was in great commotion, rising and falling in irregular waves ....

Franklin's experiment can be set up in the kitchen and completed within a minute or two, and readers are urged to try it. The instructions are given in the next paragraph (p. 439) of Franklin's letter.

> Since my arrival in America, I have repeated the experiment frequently thus. I have put a pack-thread round a tumbler, with strings of the same, from each side, meeting above it in a knot at about a foot distance from the top of the tumbler. Then putting in as much water as would fill about one third part of the tumbler, I lifted it up by the knot, and swung it to and fro in the air; when the water appeared to keep its place in the tumbler as steadily as if it had been ice. But pouring gently in upon the water about as much oil, and then again swinging it in the air as before, the tranquility before possessed by the water, was transferred to the surface of the oil, and the water under it was agitated with the same commotions as at sea.

Perhaps the first explanation of an oceanic phenomenon in terms of internal waves was V. Bjerknes' explanation of "dead water," a hitherto mysterious effect in which ships in certain coastal localities would be unable to maintain their normal speed. Ekman (1904) cites a large number of examples of the phenomenon going back as far as Pliny the Naturalist, who reported that the effect was attributed either to a mollusk or a certain type of fish that attached itself to the keel. In a preface to Ekman's paper (p. III), Bjerknes says:

> The present investigation of "Dead-Water" was occasioned by a letter in November 1898 from Prof. NANSEN asking my opinion on the subject. In my reply to Prof. NANSEN I remarked that in the case of a layer of fresh water resting on the top of salt water, a ship will not only produce the ordinary visible waves at the boundary between the water and the air, but will also generate invisible waves in the salt-water fresh-water boundary below; I suggested that the great resistance experienced by the ship was due to the work done in generating these invisible waves.

Ekman substantiated this view with extensive laboratory experiments, and includes photographs of his experiments (an example is shown in Fig. 6.2b) and slick patterns behind ships. Figure 6.2a shows such a pattern observed off British Columbia, where freshwater from river outflow forms a relatively light upper layer over the heavier salt water. The internal waves on the interface are associated with horizontal movements at the surface that affect the ripple pattern and thus become visible. The motion of the interface that corresponds to this sort of situation can be seen in Ekman's laboratory experiment (Fig. 6.2b). A nice demonstration is also given in a cine film by Long [see National Committee for Fluid Mechanics Films (1972, pp. 136–142)].

The main result of this section is that the motion can be represented in terms of two normal modes, and for each mode η satisfies the wave equation (6.2.12), i.e., the same equation as that for a homogeneous fluid (but with a different time scale). Thus the results of Chapter 5 for shallow-water motion can be applied equally well to the two-layer system. For instance, Fig. 6.3 shows the structure of the *progressive waves* associated with the two different modes in a particular case. The value of g'/g has been chosen to be small but still much larger than for the ocean. This has been done so that certain features peculiar to internal motion would be visible in the diagram, namely, the slight differences in velocity between the two layers in the "barotropic" mode of motion and the free surface movement associated with the baroclinic motion. In the ocean, the free surface movement associated with the baroclinic mode is only about 1/400 of the interface movement, but this is still sufficient for baroclinic motions to be detectable by sea-level changes (Wunsch and Gill, 1976).

Figure 6.3 shows the variation in space of a progressive internal wave at a fixed time, but the variation in time at a fixed point has the same character. For comparison Fig. 6.4 shows simultaneous observations [from Lee (1961)] of the motion of an isotherm at three points about 170 m apart, thus giving some information about variations in space as well as time. Since particles conserve their temperature over

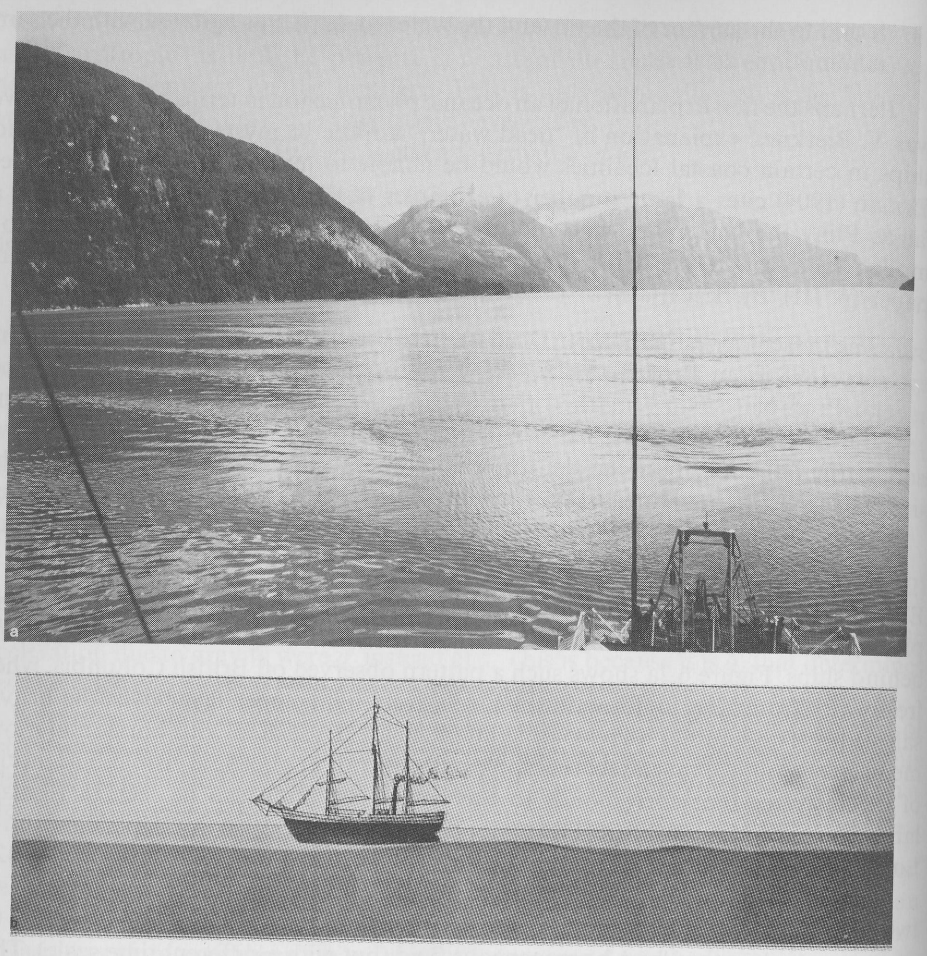

Fig. 6.2. (a) Surface "slicks" showing the presence of internal waves in the wake of a ship in Bute Inlet, British Columbia. The vessel was traveling at 0.5 m s^{-1} in a surface layer of almost fresh water only slightly deeper than its 3.4 m draft. The internal waves caused horizontal motion at the surface that affects the ripple pattern and so renders the internal wave pattern visible at the surface during calm conditions. [Photo courtesy of Defence Research Establishment Pacific, Victoria, British Columbia.] (b) A laboratory experiment [from Ekman (1904)], showing internal waves being generated by a model ship. The tank is filled with two fluids of different density, the heavier one being dyed to make the interface clearly visible. The model ship (the superstructure of the "Fram" has been drawn in subsequently) is towed from right to left, causing a wake of waves on the interface.

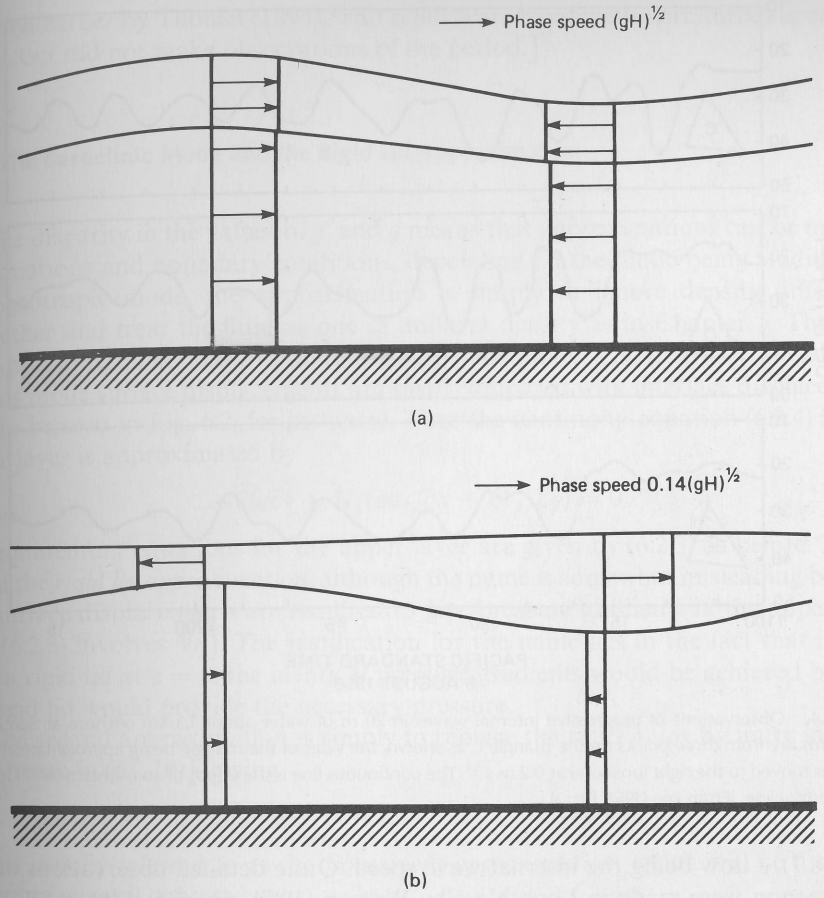

Fig. 6.3. Layer configuration in a two-layer system for a barotropic wave (a) and a baroclinic wave (b) propagating from left to right. For the case shown, the lower layer is three times deeper than the upper layer and has density 10% greater. Also shown are the directions of flow at troughs and crests, and the relative velocities of the two layers at these points.

the short period of the record, these contours mark the vertical excursion of fluid particles. Although there is in reality a continuous change of temperature with depth, the dominant features of the motion are close to those displayed by a system with two layers of different density. La Fond (1962) summarizes the main features observed at the site of these observations, where the water is 20 m deep. The period of the waves is mainly in the range 4–10 min. Since $g' \approx 0.01$ m s^{-2} and H_1 is 3–10 m, (6.2.20) gives c_1 as 0.15–0.22 m s^{-1}. This agrees well with the speed of the waves as observed by the movement of slicks and by taking simultaneous measurements at three locations. In 80% of the cases, the surface slick was found to be located between a crest and the following trough, where Fig. 6.3 shows the surface velocity field is convergent. This convergence is presumed to be responsible for the slicks.

Another extension of the results of Chapter 5 is to internal seiches and tides in channels, gulfs, and lakes. These have the form of a standing wave as given by (5.8.6)

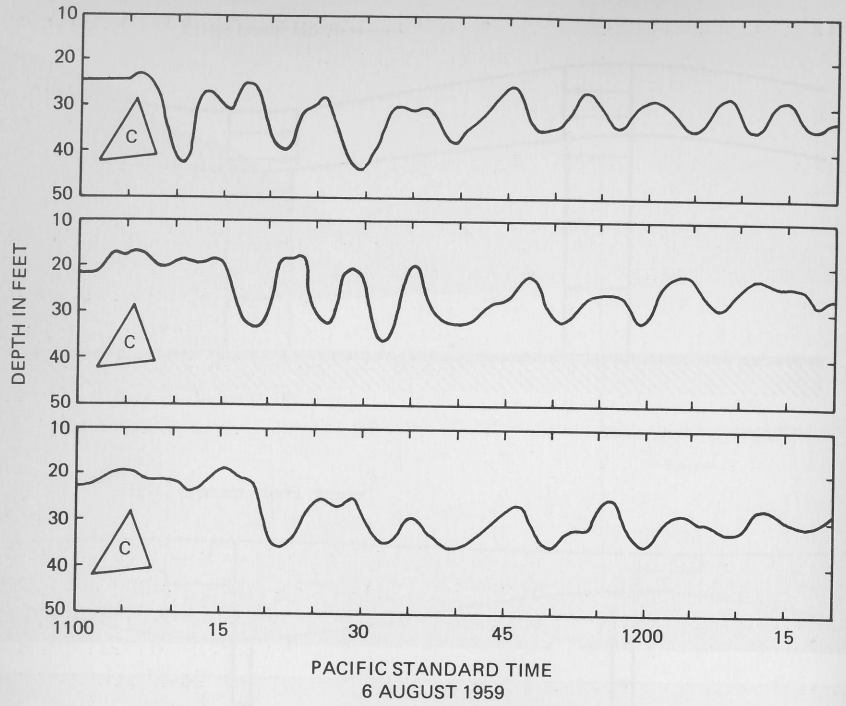

Fig. 6.4. Observations of progressive internal waves in 20 m of water about 1.3 km offshore at San Diego. The records are from three points on the triangle C as shown, the sides of the triangle being approximately 170 m. The waves moved to the right (onshore) at 0.2 m s^{-1}. The continuous line is the depth of an isotherm (64°F) located in the thermocline. [From Lee (1961, Fig. 3).]

and (5.8.7), c now being the internal wave speed. Quite detailed observations of this phenomenon were made in Loch Ness by Watson (1904, pp. 435–436).

> These observations revealed a pendulous swinging of the ends of the isotherms, the amplitude of the swing being greatest for the isotherm in the region 200 feet below the surface, and dying off both above and below this region. A few other observations taken simultaneously with these at other parts of the loch show that the isotherms are swinging as a whole about a transverse central axis.
>
> To what can this swinging be due?
>
> If we take a long rectangular trough with glass sides, and put into it a layer of water, and above the water a layer of lighter oil, and then disturb the arrangement, one of the movements observed will be a swinging of the interface between the oil and water.... The time of swing can be calculated from the formula....

The formula given is the standing-wave period, namely, twice the time to travel the length of the lake at speed c_1, given by the first term of (6.2.20). Using values of $g' \approx 2.6 \times 10^{-3}$ m s^{-2}, $H_1 \approx 60$ m, $H_2 \approx 120$ m, and a length of 40 km, Watson obtained a period of 68 hr, "which is of the same order as the period observed." He also explained how seiches could be generated by wind action, and continued even during a prolonged period of calm. [See also Watson (1903). Internal seiches were

reported earlier by Thoulet (1894), who reports an experiment with three superposed layers, but did not make observations of the period.]

6.3 The Baroclinic Mode and the Rigid Lid Approximation

The disparity in the values of g' and g means that approximations can be made to the equations and boundary conditions, depending on the mode being studied. For the barotropic mode, the approximation is simply to ignore density differences altogether and treat the fluid as one of uniform density as in Chapter 5. There are two approximations used to obtain the *baroclinic* mode. The first uses the fact that for this mode surface displacements are *small* compared with interface displacements (as can be seen in Fig. 6.2, for instance). Thus the continuity equation (6.2.4) for the upper layer is approximated by

$$-\partial h/\partial t + H_1(\partial u_1/\partial x + \partial v_1/\partial y) = 0. \tag{6.3.1}$$

The momentum equations for the upper layer are given by (6.2.3) as before. This is called the *rigid lid approximation*, although the name is somewhat misleading because free surface displacements are required to give pressure gradients in the upper layer [i.e., (6.2.3) involves $\nabla\eta$]. The justification for the name lies in the fact that if there *were* a rigid lid at $z = 0$, the identical pressure gradients would be achieved because the rigid lid would provide the necessary pressure.

The second approximation is simply to replace the ratio ρ_1/ρ_2 by unity in (6.2.7) [and hence in (6.2.10)], giving

$$\partial u_2/\partial t = -g\,\partial\eta/\partial x - g'\,\partial h/\partial x, \qquad \partial v_2/\partial t = -g\,\partial\eta/\partial y - g'\,\partial h/\partial y. \tag{6.3.2}$$

This is usually referred to as the *Boussinesq approximation*, which will be discussed in a more general context later.

Since the two continuity equations (6.3.1) and (6.2.9) do not involve η, it is desirable to obtain a combination of the momentum equations that does not involve η. This combination is obtained by subtracting (6.3.2) from (6.2.3), giving

$$\partial\hat{u}/\partial t = g'\,\partial h/\partial x, \qquad \partial\hat{v}/\partial t = g'\,\partial h/\partial y, \tag{6.3.3}$$

where $(\hat{u}, \hat{v})$ is given by

$$\hat{u} = u_1 - u_2, \qquad \hat{v} = v_1 - v_2, \tag{6.3.4}$$

and so represents the *difference in velocity* between the two layers. $(\hat{u}, \hat{v})$ can also be thought of as the amplitude of the baroclinic mode.

Now a combination of the continuity equations that involves only $(\hat{u}, \hat{v})$ is required. This is obtained by subtracting $1/H_2$ times (6.2.9) from $1/H_1$ times (6.3.1), giving

$$-\left(\frac{1}{H_1} + \frac{1}{H_2}\right)\frac{\partial h}{\partial t} + \frac{\partial\hat{u}}{\partial x} + \frac{\partial\hat{v}}{\partial y} = 0. \tag{6.3.5}$$

Equations (6.3.3) and (6.3.5) are, apart from multiplying constants, the same as Eqs.

(5.6.4)–(5.6.6) for the homogeneous fluid. Thus when the velocity components $\hat{u}$ and $\hat{v}$ are eliminated, the result is the wave equation

$$\frac{\partial^2 h}{\partial t^2} = c_1^2\left(\frac{\partial^2 h}{\partial x^2} + \frac{\partial^2 h}{\partial y^2}\right) \equiv c_1^2 \nabla^2 h, \tag{6.3.6}$$

where

$$c_1^2 = g' H_1 H_2/(H_1 + H_2) \tag{6.3.7}$$

is the square of the speed of propagation of the baroclinic mode. This is the same value as that given by (6.2.20) in the limit as $g'/g \to 0$. An alternative form of (6.3.7) is the equation

$$\frac{1}{gH_e} = \frac{1}{g'H_1} + \frac{1}{g'H_2} \tag{6.3.8}$$

for the equivalent depth $H_e = c_1^2/g$. For typical oceanic values of $g' = 0.03$ m s^{-2}, $H_1 = 400$ m, $H_2 = 4000$ m, one finds H_e is ≈ 1 m.

6.4 Adjustments within a Continuously Stratified Incompressible Fluid

So far the study of adjustment under gravity has been restricted to a fluid that has uniform density, or to a system consisting of two immiscible fluids, each of uniform density. Particular emphasis has been placed on motions with horizontal scale large compared with that of the vertical scale. In the remainder of this chapter, the study of adjustment processes will be extended to continuously stratified fluids, i.e., fluids with continuously varying density. The scale restriction will not be made at first, although the emphasis in subsequent chapters will be on motions with relatively large horizontal scale since these contain by far the most energy.

To begin, the fluids to be considered will be restricted to a class such that the density depends only on entropy and on composition, i.e., ρ depends only on the potential temperature θ and on the concentrations of the constituents, e.g., the salinity s or humidity q. Then for fixed θ and q (or s), ρ is *independent of pressure*:

$$\rho = \rho(\theta, q). \tag{6.4.1}$$

The motion that takes place is assumed to be isentropic and without change of phase, so that θ and q are constant for a material element. Therefore

$$\frac{D\rho}{Dt} \equiv \frac{\partial \rho}{\partial \theta}\frac{D\theta}{Dt} + \frac{\partial \rho}{\partial q}\frac{Dq}{Dt} = 0. \tag{6.4.2}$$

In other words, ρ is constant for a material element *because* θ and q are, and ρ depends only on θ and q. Such a fluid is said to be *incompressible*, and because of (6.4.2), the continuity equation (4.2.3) becomes (4.10.12), i.e.,

$$\partial u/\partial x + \partial v/\partial y + \partial w/\partial z = 0. \tag{6.4.3}$$

The equilibrium state to be perturbed is the state of rest, so the distribution of density and pressure is the hydrostatic equilibrium distribution given by (4.5.17) and (4.5.18). In the absence of rotation and of friction, the momentum equations (4.10.11) for *small* perturbations p' in pressure and ρ' in density become

$$\rho_0\, \partial u/\partial t = -\partial p'/\partial x, \qquad \rho_0\, \partial v/\partial t = -\partial p'/\partial y, \tag{6.4.4}$$

$$\rho_0\, \partial w/\partial t = -\partial p'/\partial z - \rho' g, \tag{6.4.5}$$

where $\rho_0(z)$ is the unperturbed density and g the acceleration due to gravity. For the moment, *no restriction on horizontal scale* is being made, so there are no approximations other than for that of the smallness of the perturbation. The governing equations are (6.4.3)–(6.4.5) and the linearized form of (6.4.2) appropriate to small perturbations, namely,

$$\partial \rho'/\partial t + w\, d\rho_0/dz = 0. \tag{6.4.6}$$

Calculations based on these equations were made by Rayleigh (1883, p. 170) "in order to illustrate the theory of cirrous clouds propounded by the late Prof. Jevons."

The initial step in dealing with the equations is the same as that used for the one- and two-layer system, namely, to eliminate u, v from the horizontal part of the momentum equations and the continuity equation. This is done by using (6.4.4) to substitute expressions for the acceleration components in the time derivative of (6.4.3). The result is

$$\rho_0 \frac{\partial^2 w}{\partial z\, \partial t} = \left(\frac{\partial^2}{\partial x^2} + \frac{\partial^2}{\partial y^2}\right) p' \equiv \nabla_H^2 p'. \tag{6.4.7}$$

This equation may be thought of as a relation between the *horizontal divergence* $\partial u/\partial x + \partial v/\partial y = -\partial w/\partial z$ and the perturbation pressure p'.

For the stratified system, another relation between w and p' is required. This is obtained by eliminating ρ' from (6.4.5) and (6.4.6) to give

$$\partial^2 w/\partial t^2 + N^2 w = -\rho_0^{-1}\, \partial^2 p'/\partial z\, \partial t, \tag{6.4.8}$$

where $N(z)$ is a quantity of fundamental importance to this problem (see Section 3.7.1 for expressions for N), defined by

$$N^2 = -g\rho_0^{-1}\, d\rho_0/dz. \tag{6.4.9}$$

N has the dimensions of frequency, and is variously known as the Brunt–Väisälä frequency, the Brunt frequency [after Brunt (1927)], the Väisälä frequency [after Väisälä (1925)], and the *buoyancy frequency* [see, e.g., Turner (1973)]. Other names (such as stability frequency and intrinsic frequency) have also been used, but Brunt–Väisälä seems to be the most common appellation. However, Rayleigh (1883) drew attention to this frequency (as the maximum possible in a stratified layer) well before Brunt and Väisälä, and buoyancy frequency is the most appropriate name physically. This is because of the solution for purely vertical motion for which p' vanishes, and hence (6.4.8) shows that the frequency of oscillation is N. The restoring force that produces the oscillation is the buoyancy force [see (6.4.5)].

There are now two equations to be satisfied, namely, (6.4.7) and (6.4.8). It is useful to think of (6.4.7) as being associated with the *horizontal* part of the motion since it is derived from the horizontal part of the momentum equations, and to think of (6.4.8) as being associated with the *vertical* part of the motion since it comes from the vertical component (6.4.5) of the momentum equation. When p' is eliminated, a single equation for w results, namely,

$$\frac{\partial^2}{\partial t^2}\left[\frac{\partial^2}{\partial x^2}+\frac{\partial^2}{\partial y^2}+\frac{1}{\rho_0}\frac{\partial}{\partial z}\left(\rho_0\frac{\partial}{\partial z}\right)\right]w+N^2\left(\frac{\partial^2}{\partial x^2}+\frac{\partial^2}{\partial y^2}\right)w=0. \tag{6.4.10}$$

It is this equation that determines how small amplitude adjustments within a continuously stratified incompressible fluid take place.

Exact solutions can be found in special cases such as those in which the density varies exponentially with height. However, there is a simplifying approximation that is always a good one in the ocean and that is valid for many applications to the atmosphere. This is based on the observation that if w varies with z much more rapidly than ρ_0, then

$$\frac{1}{\rho_0}\frac{\partial}{\partial z}\left(\rho_0\frac{\partial}{\partial z}\right)w\approx\frac{\partial^2 w}{\partial z^2}, \tag{6.4.11}$$

and so (6.4.10) can be approximated by

$$\frac{\partial^2}{\partial t^2}\left[\frac{\partial^2}{\partial x^2}+\frac{\partial^2}{\partial y^2}+\frac{\partial^2}{\partial z^2}\right]w+N^2\left(\frac{\partial^2}{\partial x^2}+\frac{\partial^2}{\partial y^2}\right)w=0. \tag{6.4.12}$$

In the ocean, ρ_0 never departs by more than 2% from its mean value, so it is a very good approximation to treat ρ_0 as a constant as implied by (6.4.11).

Another way of stating the condition for (6.4.11) to be valid is that the vertical scale for variations of w be small compared with the vertical scale for variations of ρ_0, i.e., be small compared with the *scale height* H_s (see Section 3.5). If this condition is satisfied, it turns out, as will be shown later, that (6.4.12) is a good approximation even when the fluid is compressible (conversely, if the condition is not satisfied, compressibility should *not* be ignored). Since vertically propagating internal waves in the atmosphere are usually found to satisfy this condition, (6.4.12) can be used in applications to the atmosphere as well.

The approximation that applies when the motion has vertical scale small compared with the scale height is called the *Boussinesq approximation* [see, e.g., Spiegel and Veronis (1960)] and is attributed to Boussinesq (1903). Basically, it consists of taking the density to be constant in computing rates of change of momentum from accelerations, but taking full account of density variations when they give rise to *buoyancy* forces, i.e., when there is a multiplying factor g in the vertical component of the momentum equations. For the case considered in this chapter, this means taking ρ_0 as a constant in (6.4.4) and (6.4.5) and hence in (6.4.7) and (6.4.8). Buoyancy effects come in through the term $\rho' g$ in (6.4.5), which gives rise to the term $N^2 w$ in (6.4.8).

6.5 Internal Gravity Waves

Consider the case in which the buoyancy (Brunt–Väisälä) frequency N is constant throughout the fluid. Traveling wave solutions of (6.4.12) can be found of the form

$$w=w_0\cos(kx+ly+mz-\omega t), \tag{6.5.1}$$

where w_0 is the *amplitude* of vertical velocity fluctuations, the vector

$$\mathbf{k}=(k,l,m) \tag{6.5.2}$$

is the *wavenumber* of the disturbance, and ω is the frequency. In order for (6.5.1) to satisfy Eq. (6.4.12), ω and $\mathbf{k}$ must be related by the *dispersion relation*

$$\omega^2=(k^2+l^2)N^2/(k^2+l^2+m^2). \tag{6.5.3}$$

Thus internal waves can have any frequency between zero and a *maximum* value of N. As Rayleigh (1883, p. 174) put it, "Contrary to what is met with in most vibrating systems, there is a limit on the side of rapidity of vibration, but none on the side of slowness."

The dispersion relation for internal waves is of quite a different character compared to that for surface waves. In particular, the frequency of surface waves depends only on the *magnitude* κ of the wavenumber, whereas the frequency of internal waves is *independent* of the magnitude of the wavenumber and depends only on the *angle* φ' that the wavenumber vector makes with the horizontal. To bring this out, it is useful to specify the wavenumber in spherical polar coordinates $(\lambda', \varphi', \kappa)$ in wavenumber space (see Fig. 6.5), namely,

$$k=\kappa\cos\varphi'\cos\lambda',\qquad l=\kappa\cos\varphi'\sin\lambda',\qquad m=\kappa\sin\varphi'. \tag{6.5.4}$$

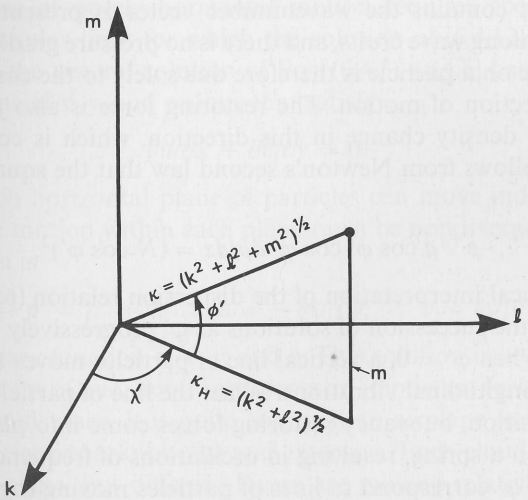

Fig. 6.5. The system of spherical polar coordinates in wavenumber space used to express the dispersion relation for internal waves. For these waves, the frequency ω does not depend on the magnitude κ of the wavenumber but only on the direction φ' between the wavenumber and the horizontal plane. The dispersion relation is $\omega = N\cos\varphi'$.

The prime is used to denote wavenumber angles as opposed to angles in physical space. Then the dispersion relation (6.5.3) becomes simply

$$\omega = N \cos \varphi'. \tag{6.5.5}$$

The way p', ρ', u, and v vary for the plane wave (6.5.1) can be deduced from the appropriate equations. The relationships among these variables are sometimes called the *polarization relations*. The perturbation pressure p' is, from (6.4.7), given by

$$p' = -(k^2 + l^2)^{-1}\omega m \rho_0 w_0 \cos(kx + ly + mz - \omega t), \tag{6.5.6}$$

whereas (6.4.6) gives for the perturbation density

$$\rho' = -(N^2/\omega g)\rho_0 w_0 \sin(kx + ly + mz - \omega t). \tag{6.5.7}$$

Note that the last two equations, together with (6.5.3), imply that for a plane progressive wave,

$$\partial p'/\partial z = -(m^2/(k^2 + l^2 + m^2))g\rho'. \tag{6.5.8}$$

The horizontal velocity components can be found from (6.4.4), which gives

$$\begin{aligned}(u, v) &= -(k, l)(k^2 + l^2)^{-1}\, m w_0 \cos(kx + ly + mz - \omega t) \\ &= (k, l)(\omega\rho_0)^{-1} p'.\end{aligned} \tag{6.5.9}$$

The above relations between pressure and velocity fluctuations can be useful for deducing wave properties from observations at a fixed point. For instance, if the horizontal velocity components and perturbation pressure of a progressive wave are measured, the horizontal component of the wavenumber vector can be deduced from (6.5.9). This device was used, for instance, by Gossard and Munk (1954).

A sketch showing the properties of a plane progressive internal wave in the vertical plane that contains the wavenumber vector is presented in Fig. 6.6. The particle motion is along wave crests, and there is no pressure gradient in this direction. The restoring force on a particle is therefore due solely to the component $g \cos \varphi'$ of gravity in the direction of motion. The restoring force is also proportional to the component of the density change in this direction, which is $\cos \varphi'\, d\rho/dz$ per unit displacement. It follows from Newton's second law that the square of the frequency of vibration is

$$\rho^{-1} g \cos \varphi' \cos \varphi'\, d\rho/dz = (N \cos \varphi')^2,$$

thus giving a physical interpretation of the dispersion relation (6.5.5).

Consider now the succession of solutions as φ' progressively increases from zero to a right angle. When $\varphi' = 0$, a vertical line of particles moves together like a rigid wire undergoing longitudinal vibrations. When the line of particles is displaced from its equilibrium position, buoyancy restoring forces come into play just as if the line of particles were on a spring, resulting in oscillations of frequency N. The solutions for other values of φ' correspond to lines of particles moving together at angle φ' to the vertical. The restoring force per unit displacement is less than it is for $\varphi' = 0$, and so the frequency of vibration is less. As φ' tends to $\pi/2$, the frequency of vibration tends to zero.

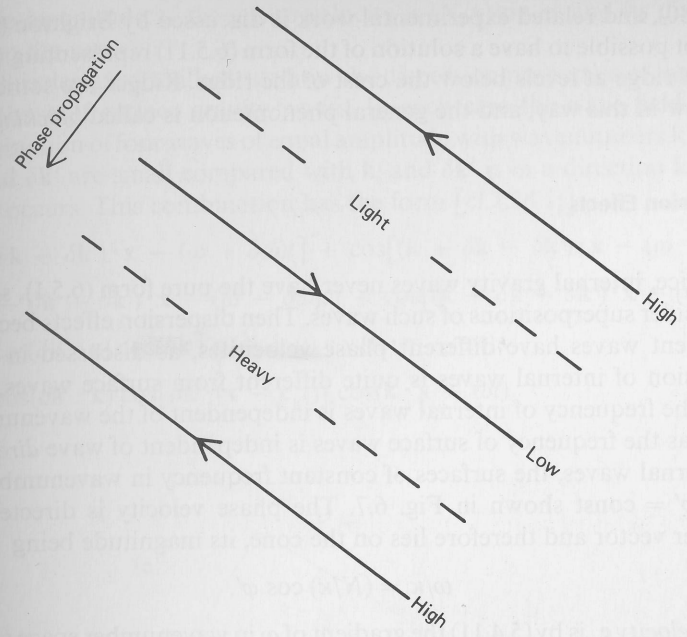

Fig. 6.6. Sketch showing in a vertical plane the phase relationships for a progressive internal wave with downward phase velocity (this implies upward group velocity). The solid lines mark lines of maximum (High) and minimum (Low) pressure, which are also lines of maximum and minimum velocity, the direction of motion being as shown. The dashed lines mark the positions of maximum (Heavy) and minimum (Light) density perturbations. If the direction of phase propagation is reversed, the only change in the diagram is a reversal of the direction of motion.

The extreme case of purely horizontal motion requires special consideration because this is a singular limit for which the solution of (6.4.12) is the trivial one, $w = 0$. In this case, the general solution of Eqs. (6.4.3)–(6.4.6) has $p' = \rho' = 0$, with u and v any functions of x, y, and z alone that satisfy

$$\partial u/\partial x + \partial v/\partial y = 0. \tag{6.5.10}$$

In other words, each horizontal plane of particles can move independently of any other plane, but the motion within each plane must be nondivergent. An alternative form of this solution is

$$w = p' = \rho' = 0, \qquad u = -\partial\psi/\partial y, \qquad v = \partial\psi/\partial x, \tag{6.5.11}$$

where ψ is an arbitrary function of x, y, and z. This solution is *not* an internal wave, or even a limiting form of one, but it represents an important form of motion that is often observed. For instance, it is quite common an airplane journeys to see thick layers of cloud that are remarkably flat and extensive. Each cloud layer is moving in its own horizontal plane, but different layers are moving relative to each other as described by (6.5.11). If a mountain pierces such a layer, it is possible to have motion of the form (6.5.11) with two-dimensional flow around the mountain in each horizontal layer. Spectacular consequences are the vortex streets observed behind islands

(Gjevik, 1980), and related experimental work is discussed by Brighton (1978). However, it is not possible to have a solution of the form (6.5.11) representing uniform flow normal to a ridge at levels below the crest of the ridge. Ridges are sometimes found to block flow in this way, and the general phenomenon is called *blocking*.

6.6 Dispersion Effects

In practice, internal gravity waves never have the pure form (6.5.1), so it is necessary to consider superpositions of such waves. Then dispersion effects become evident when different waves have different phase velocitites, as discussed in Section 5.4. The dispersion of internal waves is quite different from surface waves, one reason being that the frequency of internal waves is independent of the wavenumber *magnitude*, whereas the frequency of surface waves is independent of wave *direction*.

For internal waves, the surfaces of constant frequency in wavenumber space are the cones $\varphi' = \text{const}$ shown in Fig. 6.7. The phase velocity is directed along the wavenumber vector and therefore lies on the cone, its magnitude being

$$\omega/\kappa = (N/\kappa)\cos\varphi'.$$

The *group velocity* $\mathbf{c}_g$ is by (5.4.11) the gradient of ω in wavenumber space and therefore is normal to the surface of constant ω. It follows that (as for any waves whose frequency is independent of wavenumber magnitude) the group velocity is at right angles to the wavenumber vector. When the group velocity has an upward component, therefore, the phase velocity has a downward component, and vice versa. By (5.4.11)

$$\mathbf{c}_g = (N/\kappa)\sin\varphi'(\sin\varphi'\cos\lambda', \sin\varphi'\sin\lambda', -\cos\varphi'). \tag{6.6.1}$$

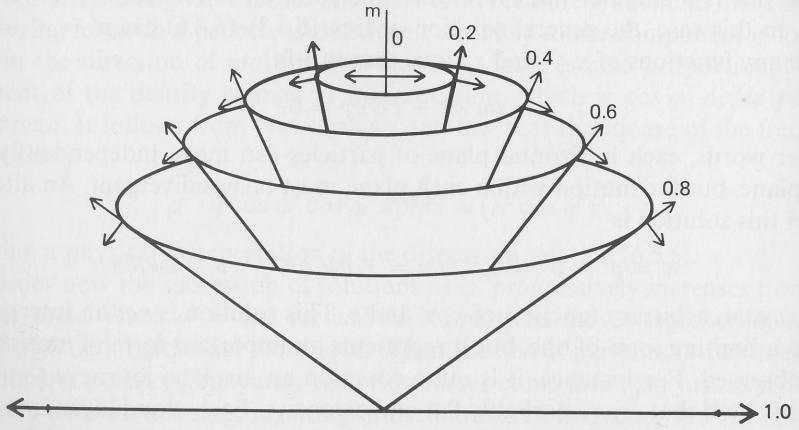

Fig. 6.7. For internal waves (no rotation), the surfaces of constant frequency in wavenumber space are cones as shown, contours being values of ω/N, where ω is the frequency and N the buoyancy frequency. The group velocity is in a direction perpendicular to the cone in the direction of increasing frequency as shown by one set of arrows, whereas the phase velocity is in a direction along the cone away from the origin as shown by the other set of arrows.

Therefore the magnitude of the group velocity is $(N/\kappa)\sin\varphi'$ and its direction is at an angle φ' to the *vertical*.

Figure 6.8 is designed to illustrate how the dispersion properties of internal waves differ from those of surface gravity waves. In each case the wave field shown is a simple combination of four waves of equal amplitude with wavenumbers $\mathbf{k} \pm \delta\mathbf{k} \pm \delta\mathbf{k}'$, where $\delta\mathbf{k}$ and $\delta\mathbf{k}'$ are small compared with $\mathbf{k}$, and $\delta\mathbf{k}'$ is in a direction for which no change in ω occurs. This combination has the form [cf. (5.4.1)]

$$\begin{aligned}&\cos[(\mathbf{k}+\delta\mathbf{k}+\delta\mathbf{k}')\cdot\mathbf{x}-(\omega+\delta\omega)t] + \cos[(\mathbf{k}+\delta\mathbf{k}-\delta\mathbf{k}')\cdot\mathbf{x}-(\omega+\delta\omega)t]\\ &+\cos[(\mathbf{k}-\delta\mathbf{k}+\delta\mathbf{k}')\cdot\mathbf{x}-(\omega-\delta\omega)t] + \cos[(\mathbf{k}-\delta\mathbf{k}-\delta\mathbf{k}')\cdot\mathbf{x}-(\omega-\delta\omega)t]\\ &\quad = 4\cos(\delta\mathbf{k}'\cdot\mathbf{x})\cos(\delta\mathbf{k}\cdot\mathbf{x}-\delta\omega t)\cos(\mathbf{k}\cdot\mathbf{x}-\omega t)\\ &\quad \approx 4\cos(\delta\mathbf{k}'\cdot\mathbf{x})\cos[\delta\mathbf{k}\cdot(\mathbf{x}-\mathbf{c}_g t)]\cos(\mathbf{k}\cdot\mathbf{x}-\omega t).\end{aligned} \tag{6.6.2}$$

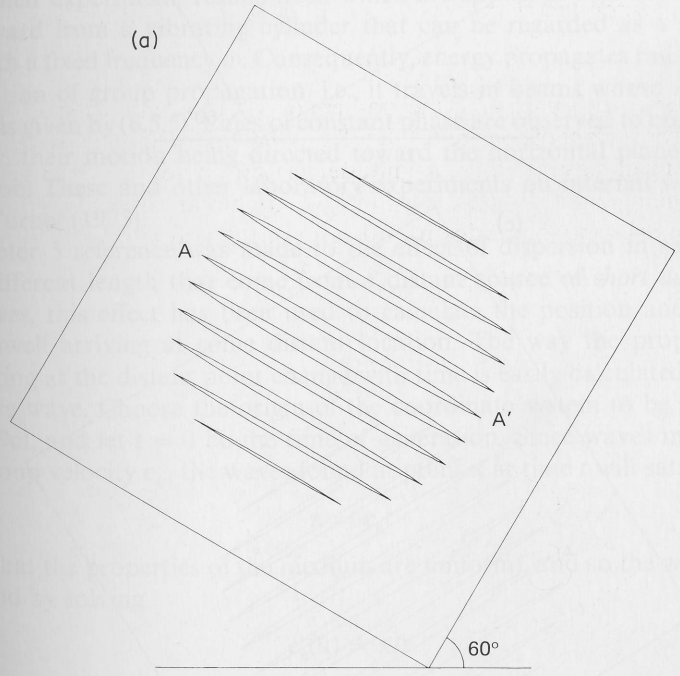

Fig. 6.8. A contrast between the dispersion characteristics of internal waves and surface gravity waves, illustrated by the behavior of a suitable combination of four progressive waves. (a) The initial configuration of a group of internal waves with wave crests at 60° to the vertical. Contours are of pressure perturbation, where this is equal to +0.5 times the maximum value. (b) The configuration four periods later, the group having moved parallel to the crests and upward, while the individual crest AA' has moved four wavelengths downward and to the left. To compare this with the way surface waves behave, suppose (a) now shows a plan view of a similar combination of waves, contours now being where the surface elevation is +0.5 times the maximum value. Then (b) shows the configuration four periods later. The individual wave crest AA' has again moved four wavelengths, but now the group has moved two wavelengths in the same direction.

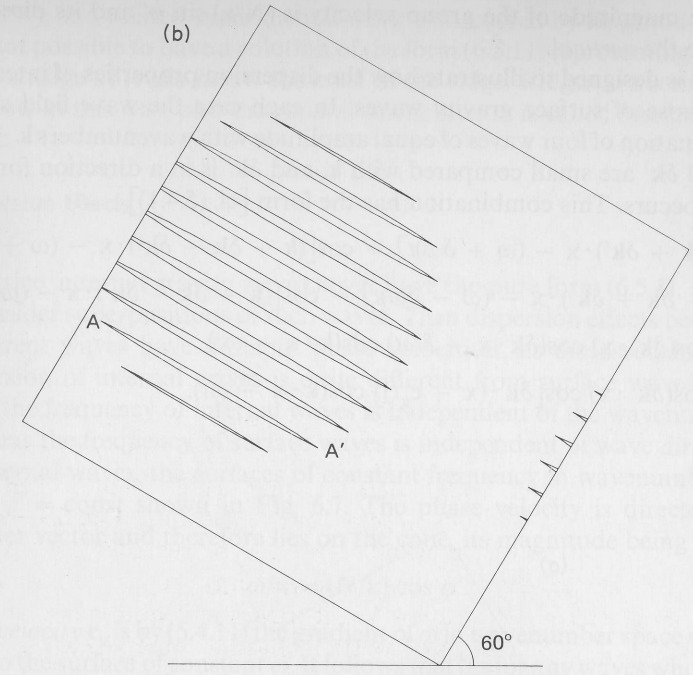

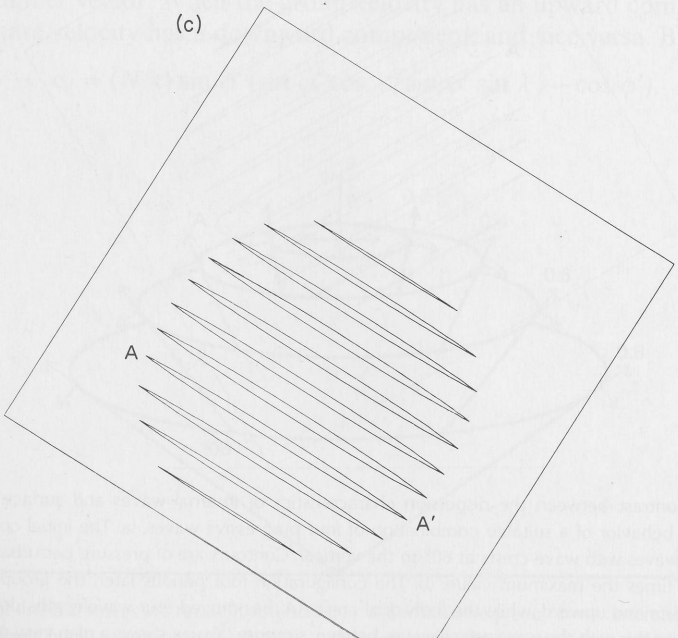

Fig. 6.8. (*continued*)

Figure 6.8a represents such a combination of internal gravity waves. It is a vertical section in the plane of propagation, showing contours only where the pressure perturbation is $+0.5$ times the maximum value for the whole wave field. The wavenumber vector is at angle $\varphi' = 60°$ to the vertical and pointing downward, $\delta\mathbf{k}'$ is chosen to be equal to $0.03\mathbf{k}$, and $\delta\mathbf{k}$ has the same magnitude but is at right angles to $\delta\mathbf{k}'$. Figure 6.8b shows the same waves four periods later. Wave crest AA' has moved four wavelengths downward to the left, but the wavegroup has moved upward parallel to the crests, i.e., at right angles to the direction of phase propagation, For comparison, Fig. 6.8c shows the behavior of a similar combination of surface gravity waves. In this case, Fig. 6.8a is interpreted as a plan view, showing contours of surface elevation, with $\delta\mathbf{k} = 0.03\mathbf{k}$ and $\delta\mathbf{k}'$ of the same magnitude but at right angles. Figure 6.8c is the view four periods later, crest AA' having moved four wavelengths. The group as a whole has moved in the same direction but at half the speed.

The difference in the directions of phase and group propagation for internal waves is nicely illustrated in laboratory experiments (Mowbray and Rarity, 1967), in which density perturbations can be made visible by using shadowgraph or Schlieren techniques. In their experiment, results from which are shown in Fig. 6.9, energy propagates outward from a vibrating cylinder that can be regarded as a point source of waves with a fixed frequency ω. Consequently, energy propagates radially outward in the direction of group propagation, i.e., it travels in beams whose angle φ' with the *vertical* is given by (6.5.5). Lines of constant phase are observed to cross the beams transversely, their motion being directed toward the horizontal plane through the source region. These and other laboratory experiments on internal waves are discussed by Turner (1973).

In Chapter 5 reference was made to the effect of dispersion in separating out waves of different length that come from a distant source of *short duration*. With surface waves, this effect has been used to calculate the position and time of the source of swell arriving at some distant location. The way the properties of the waves arriving at the distant point change with time is easily calculated for *any* type of dispersive wave. Choose the origin of the coordinate system to be at the source (see Fig. 6.9c), and let $t = 0$ be the time of generation. Since waves move outward with the group velocity $\mathbf{c}_g$, the waves found at point $\mathbf{x}$ at time t will satisfy

$$\mathbf{x} = \mathbf{c}_g t$$

(provided that the properties of the medium are uniform), and so the wavenumber $\mathbf{k}$ can be found by solving

$$\mathbf{c}_g(\mathbf{k}) = \mathbf{x}/t. \tag{6.6.3}$$

Consider the special case of internal waves in which $\mathbf{c}_g$ is given by (6.6.1) and hence $O\mathbf{x}$ makes angle φ' with the vertical. Since this angle is fixed for a given point $\mathbf{x}$ of observation, the frequency ω of the waves passing this point will have the fixed value given by (6.5.5). In other words, wave crests will pass at fixed intervals of time. However, the spacing between crests will decrease with time; for (6.6.3) gives (for magnitudes)

$$c_g = r/t,$$

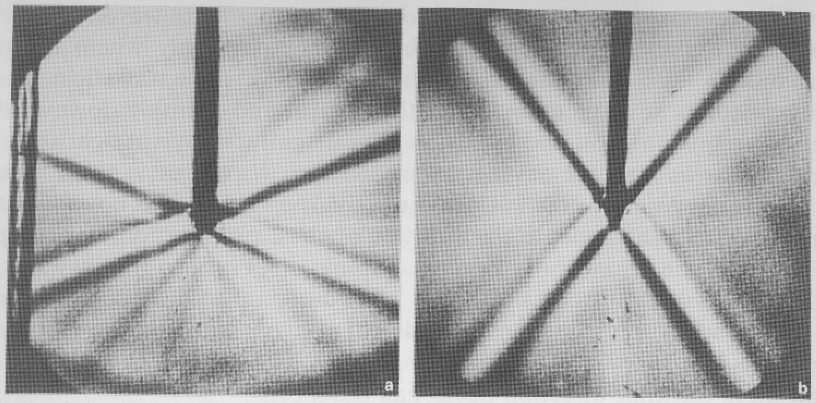

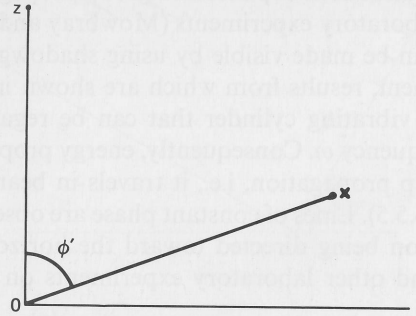

(c)

Fig. 6.9. Patterns, obtained by Schlieren techniques, of internal waves propagating away from a cylinder that is vibrating at a frequency given by (a) $\omega/N = 0.366$, (b) $\omega/N = 0.699$. Waves propagate outward with group velocity along the dark lines, which indicate an extreme of refractive index and hence a wave crest. The orientation of the crest is the one expected for the frequency of vibration. The dark lines continually move toward the horizontal plane containing the cylinder, new lines appearing at the top edge of the beam and old ones disappearing at the lower edge of the beam, thus showing that the phase propagation is at right angles to the group velocity. [From D. E. Mowbray and B. S. H. Rarity (1967). A theoretical and experimental investigation of the phase configuration of internal waves of small amplitude in a density stratified fluid. *J. Fluid Mech.* **28,** 1 (Plate 1). Cambridge University Press.] (c) The geometry of the situation. For a point source at O, waves received at $\mathbf{x}$ travel in the direction of the group velocity, and hence $\mathbf{c}_g$ is in the direction of $O\mathbf{x}$. The angle marked is ϕ' since $\mathbf{c}_g$ makes this angle to the vertical. ϕ' is also the angle the wavenumber vector makes with the horizontal since the phase velocity is at right angles to the group velocity. For a source of fixed frequency ω as in the experiments shown in (a) and (b), waves are observed only along the beam for which ϕ' is given by (6.5.5). For an impulsive source applied at $t = 0$, all frequencies will be present, but only those with frequency ω, given by (6.5.5), will be observed at $\mathbf{x}$. The wavenumber of the dominant wave will, however, increase with time as calculated in the text.

and substitution for c_g from (6.6.1) then gives

$$\kappa = r^{-1}Nt \sin \varphi'. \tag{6.6.4}$$

Thus κ increases in proportion with time, i.e., the spacing between wave crests decreases inversely in proportion with time. More detailed discussion of the solution for an impulsive source of internal waves is given by Bretherton (1967), and further discussion of the general problem is given by Whitham (1974) and Lighthill (1978).

Sometimes geometric factors cause the wavenumber to be constrained to lie on some surface or line in wavenumber space, in which case the dispersion properties depend on how the frequency varies on that surface or line. For example, the vertical component m of the wavenumber may be fixed because the waves are contained in a region of finite vertical extent. The dispersion properties then depend on how ω, given by (6.5.3), varies with k and l. This shows that the long waves, which have low frequency, have the largest group velocity, equal to N/m. As the horizontal component of wavenumber increases, the frequency increases toward a maximum value of N and the group velocity decreases toward zero. (Further discussion of this case can be found in Section 6.10.)

Another example corresponds to the case in which the horizontal component (k, l) of the wavenumber is fixed, so that (6.5.3) is regarded as a relation between ω and m. In this case, the frequency is a maximum and the group velocity c_{gz} is zero when $m = 0$. The group velocity also tends to zero as $m \to \infty$, and has a maximum at a value of m, corresponding to propagation at 35° to the vertical ($\cot \varphi' = 2^{1/2}$). The associated frequency is $(2/3)^{1/2}N$ and the group velocity is $2N/3^{3/2}(k^2 + l^2)^{1/2}$.

6.7 Energetics of Internal Waves

The energy equation for internal waves can be obtained by multiplying (6.4.4) by (u, v), (6.4.5) by w, and (6.4.6) by $g^2\rho'/\rho_0 N^2$, then adding the results. With the use of (6.4.3) and (6.4.9), this gives

$$\frac{\partial}{\partial t}\left[\frac{1}{2}\rho_0(u^2 + v^2 + w^2) + \frac{1}{2}\frac{g^2\rho'^2}{\rho_0 N^2}\right] + \frac{\partial}{\partial x}(p'u) + \frac{\partial}{\partial y}(p'v) + \frac{\partial}{\partial z}(p'w) = 0. \tag{6.7.1}$$

This is a special case of the total energy equation discussed in Section 4.7. As found in Chapter 4, the energy equation can be integrated over a large volume, thereby giving useful results about overall balances.

The identification of the perturbation kinetic energy density term $\frac{1}{2}\rho_0(u^2 + v^2 + w^2)$ in (6.7.1) with the corresponding term in (4.7.3) is obvious, as is the correspondence between the perturbation energy flux term $(p'u, p'v, p'w)$ in (6.7.1) and the full expression (4.7.4) for the flux when account is taken of the perturbations being infinitesimal, incompressible, inviscid, and nondiffusive. The identification of the perturbation potential energy term in (6.7.1) is less obvious, and it is helpful first to consider the case of the two-layer fluid of Section 6.2. There the potential energy (see Section 5.7) is equal to

$$\begin{aligned}\iiint \rho\Phi \, dx\, dy\, dz &= \iiint \rho g z \, dz\, dx\, dy \\ &= \iint \left\{\frac{1}{2}\rho_1 g[\eta^2 - (H_1 - h)^2] + \frac{1}{2}\rho_2 g[(H_1 - h)^2 - H^2]\right\} dx\, dy,\end{aligned}$$